Articles

A Structure-Based Design Approach to the Development of Novel, Reversible AChE Inhibitors

Caroline Doucet-Personeni,[†] Philip D. Bentley,[†] Rodney J. Fletcher,[†] Adrian Kinkaid,[†] Gitay Kryger,[‡] Bernard Pirard,[†] Anne Taylor,[†] Robin Taylor,[§] John Taylor,[†] Russell Viner,*[,†] Israel Silman,[||] Joel L. Sussman,[‡] Harry M. Greenblatt,[‡] and Terence Lewis[†]

Syngenta, Jealott's Hill Research Station, Bracknell, Berkshire RG42 6EY, U.K., Departments of Structural Biology and Neurobiology, Weizmann Institute of Science, Rehovot 76100, Israel, and Cambridge Crystallographic Data Centre, 12 Union Road, Cambridge CB2 1EZ, U.K.

Received January 19, 2001

Chimeras of tacrine and *m*-(*N*,*N*,*N*-Trimethylammonio)trifluoroacetophenone (**1**) were designed as novel, reversible inhibitors of acetylcholinesterase. On the basis of the X-ray structure of the apoenzyme, a molecular modeling study determined the favored attachment positions on the 4-aminoquinoline ring (position 3 and the 4-amino nitrogen) and the favored lengths of a polymethylene link between the two moieties (respectively 5−6 and 4−5 sp^3 atoms). Seven compounds matching these criteria were synthesized, and their inhibitory potencies were determined to be in the low nanomolar range. Activity data for close analogues lacking some of the postulated key features showed that our predictions were correct. In addition, a subsequent crystal structure of acetylcholinesterase complexed with the most active compound **27** was in good agreement with our model. The design strategy is therefore validated and can now be developed further.

Introduction

While the essential biological role of acetylcholinesterase (AChE) in the mediation of vertebrate and invertebrate nervous transmission has been known for more than 80 years, this remarkable enzyme continues to be the focus of much interest in pharmaceutical and agrochemical circles. Medicinally, it has been targeted in treatments for Alzheimer's disease, myasthenia gravis, and glaucoma, and in the recovery of victims of nerve agent exposure.[1−4] Agrochemically, AChE is the most widely exploited insecticide target: all the commercial organophosphate and carbamate agents are believed to exert their effects through irreversible inhibition of the enzyme.[5] More recently, researchers in these areas have focused on two key objectives, discovering (a) *selective* inhibitors of the mammalian enzyme for the effective treatment of Alzheimer's disease, thereby avoiding the undesirable side effects of the established drug, tacrine[6] (Figure 1), and (b) *selective* inhibitors of insect enzymes which would avoid the problems of both acute and chronic toxic effects of organophosphate (e.g., parathion) and carbamate (e.g., carbofuran) insecticides on human and other vertebrate life.[7]

The emphasis in both of these areas is on obtaining selectivity for AChE over other members of the ubiquitous family of enzymes, the serine hydrolases (e.g., esterases, ligases, amidases, proteases), which share the same catalytic mechanism. Any new commercial product would require selectivity of this nature to be both safe and successful.

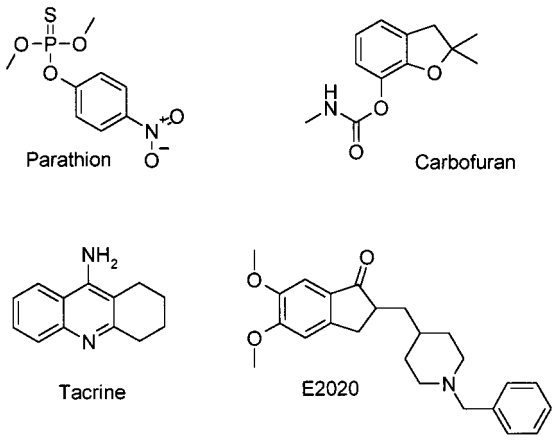

Figure 1. Examples of commercially important AChE inhibitors.

When these goals were first tackled in the 1970s and 1980s, little was known about the structure of AChE. Attempts at structure-based inhibitor design at this stage were highly speculative, and successful inhibitor discovery was driven more by "random" screening and exhaustive analogue investigation than by an understanding of inhibitor−protein interactions. Despite these challenges, the approach afforded the first truly selective, commercially viable AChE inhibitor in the form of

* To whom correspondence should be addressed: E-mail: Russell.Viner@syngenta.com. Phone: +44 1344 414180. Fax: +44 1344 455629.
[†] Syngenta.
[‡] Department of Structural Biology, Weizmann Institute of Science.
[§] Cambridge Crystallographic Data Centre.
[||] Department of Neurobiology, Weizmann Institute of Science.

10.1021/jm010826r CCC: $20.00
Published on Web 08/28/2001

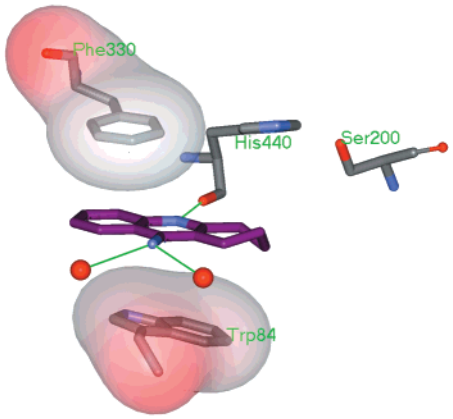

Figure 2. Tacrine−*Torpedo* AChE complex X-ray structure showing key interactions and the proximity of active site serine (Ser200). The tacrine carbon atoms are magenta; all other atoms are colored by atom type. The hydrogen bonds with the corresponding acceptor−donor distances are in green.

the anti-Alzheimer drug Aricept (E2020) in 1995 (Figure 1).[8] The elucidation of the crystal structure of *Torpedo californica* AChE (*Tc*AChE) in 1991[9] and subsequent enzyme−inhibitor complexes[10−18] has provided researchers with an invaluable tool for studying the structure and function of this enzyme.

The unusual location of the catalytic site at the base of a deep, narrow gorge lined with aromatic residues has prompted extensive investigation across a diverse range of topics, including the mechanism of substrate binding and turnover,[19,20] the role of cation−π and $\pi-\pi$ interactions,[21] the possible contribution of electrostatics in catalysis and noncholinergic functions,[22] and of course the attempted rationalization of known inhibitor binding and novel inhibitor design.[23−29]

Recently post-hoc rationalization of the binding mode of E2020 has been possible by analysis of the crystal structure of the inhibitor−*Tc*AChE complex,[14,30] which has highlighted the importance of aromatic interactions between protein and inhibitor which were largely overlooked in the original predictions.

Background

We have been studying the structure and function of AChE to design novel, reversible active site inhibitors, with a view to developing selective insecticides which would function efficiently without the potentially harmful side effects of more traditional agrochemicals. The current work was facilitated by the availability of structural information of the known anti-Alzheimer drug tacrine bound to the active site of *Torpedo* AChE (Figure 2).[31] An analysis of the complex highlighted a number of key features of the binding mode.

The inhibitor binds in its protonated form and participates in four different kinds of intermolecular interactions:

(1) H-bonding to both the protein and "structural" water molecules,

(2) aromatic ($\pi-\pi$ stacking and edge-to-face) interactions, mainly with W84 and F330,

(3) cationic nitrogen−aromatic interactions ($N^+-\pi$), mainly with W84 and F330, and

(4) hydrophobic contacts involving non-H-bonding groups of inhibitor and protein.

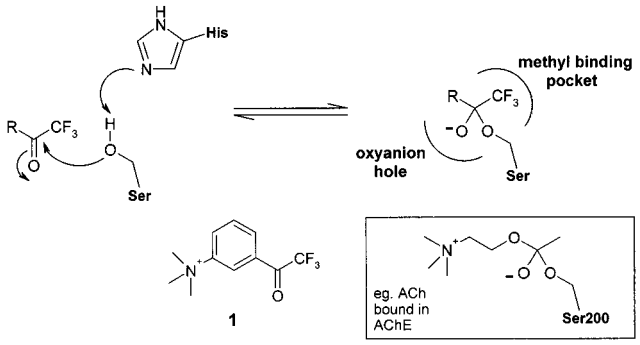

Figure 3. Binding mode of trifluoromethyl ketones at the active site of serine hydrolase enzymes, compared with acetylcholine binding to AChE.

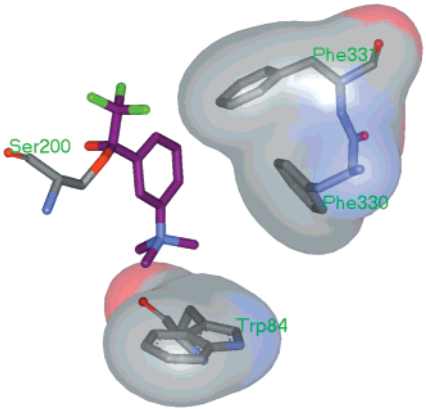

Figure 4. Model of the "Quinn inhibitor"−*Tc*AChE complex X-ray structure showing key inhibitor−protein interactions. The inhibitor carbon atoms are magenta; all other atoms are colored by atom type.

Tacrine forms only one direct H-bond with the protein, with the overall binding mode apparently dominated by aromatic and hydrophobic contacts. This mode of binding has since been shown to be important for a variety of inhibitor and substrate types. It is also worth noting that $\pi-\pi$ interactions are not usually favorable except when a charged ring system (such as the acridinium system) is involved. The inhibitor occupies only a part of the active site, while the immediate vicinity of the catalytic serine 200 is occupied by water.

Of particular interest are inhibitors which act as transition-state mimics, such as trifluoromethyl ketones. A number of examples of such compounds acting as inhibitors of serine hydrolases, including lipases,[32] proteases,[33−35] juvenile hormone esterase,[36] and AChE[36,37] are known. The substrate-like inhibitor **1** of AChE (Figure 3) studied by Quinn's group is of this class and is one of the most potent reversible inhibitors of AChE reported in the literature. Sussman, Silman, et al. confirmed the nature of the binding mode of compound **1** complexed with *Torpedo* AChE by X-ray analysis (Figure 4).[10] The active site serine covalently bonds to the activated carbonyl of the trifluoroacetyl group, while the quaternary ammonium group interacts favorably with the adjacent aromatic residues Trp84 and Phe330 among others.

Molecular Design

The overall philosophy guiding our design was to try to find a single molecule that could exhibit the trifluo-

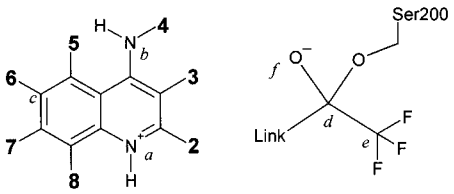

a - *d*	6.72 Å
a - *e*	7.43 Å
a - *f*	7.38 Å
b - *d*	5.87 Å
b - *e*	6.41 Å
b - *f*	5.89 Å
c - *d*	6.18 Å
c - *e*	7.44 Å
c - *f*	6.06 Å

Figure 5. Distances and linkage positions used in the design template.

roacetyl binding mode *and* the Trp84 ring stacking binding mode simultaneously. Since both of these binding modes are observed for potent inhibitors of AChE, it was hoped that combining these two effects would lead to even higher affinity ligands with greater specificity for AChE. The binding sites for the two modes appeared, by inspection of the crystal structure of the apoenzyme, to be sufficiently separate to allow both to be occupied simultaneously, while at the same time being close enough to make a bridging strategy attractive. The aim was therefore to link a 4-aminoquinoline ring (as found in the tacrine ring system) to a trifluoroacetyl group so as to span the two sites. The nature of the linkage, and its attachment position to the 4-aminoquinoline ring, remained to be determined.

A manual docking of tacrine into the crystal structure of the apoenzyme (PDB code 1ACE)[9] indicated that there was insufficient space to accommodate a chain at positions 6, 7, and 8 of the 4-aminoquinoline ring (Figure 5). However, positions 2, 3, and 5 and the 4-amino nitrogen all seemed to offer opportunities for attaching a linking group.

A computational method was used to help choose the best attachment position for the linker, as well as the correct length. A template was defined by an aminoquinoline ring stacked with Trp84 and a detached trifluoroacetyl group docked into the oxyanion hole. This template was characterized by measuring the nine distances shown in Figure 5.

Preliminary modeling work using the template suggested that the two groups could probably be linked by a chain of 3−6 sp^3 atoms, depending on the attachment position, and the extent to which the chain was folded. Twelve candidate molecules were modeled using chain lengths in this range and the four possible attachment positions, and appending a hydrated trifluoroacetyl group ($C(OH)_2CF_3$) to the end of the chain. A conformational search was carried out for each candidate molecule to identify reasonably low energy conformations where the distances in the candidate molecule best matched the distances in the template. The conformations found were then energy minimized, but with the nine distances constrained to stay near their template values. The conformations were then overlaid on the template and inspected in the active site. For each candidate molecule, the best conformation was identified, attempting to take into account the goodness of fit to the template, steric clashes with the protein, conformational strain in the ligand, and solvent accessibility of H-bonding groups in the active site. The same criteria were used to rank the molecules against each other. The favored molecules selected by this process were those with chains linked to position 3 (chains of type $-CH_2-O-(CH_2)_n$, $n = 3$ and 4) and to the 4-amino nitrogen (chains of type $-(CH_2)_m$, $m = 4$ and 5).

Synthetic targets were then designed on the basis of these preferred attachment points and chain lengths. Further rings and heteroatoms were introduced into the chains to reduce flexibility (entropic benefit) and ease the synthesis. These introductions were made so as to preserve as much as possible the required conformations of the chains, and to fit within the space constraints of the active site.

The final list of novel putative inhibitor structures, **A**−**D**, selected for synthesis is shown in Figure 6. Precedents suggest that 8-substitution of tacrine tended to increase binding so an equivalent halogen substituent was usually retained in our target molecules.[38,39]

Chemistry

From a synthetic standpoint the tacrine-like tricyclic targets **A** seemed most readily accessible. A successful route to this class of compounds is outlined in Scheme 1. Alkylation of the known tacrine derivative **2** with

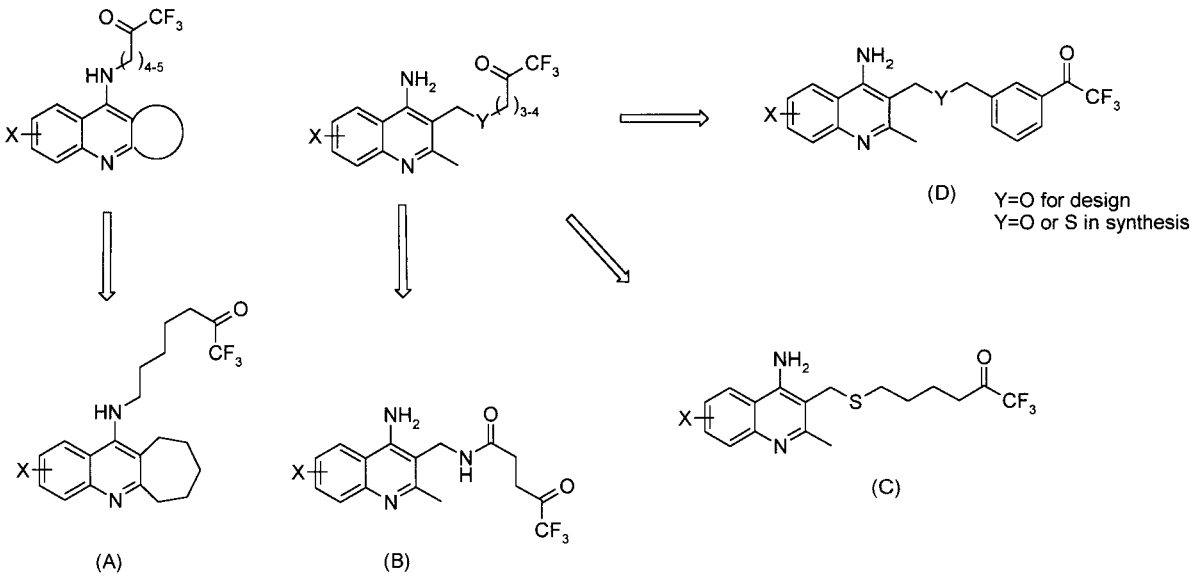

Figure 6. Structural types of inhibitors suggested by the computational approach, and some resulting synthetic targets.

Scheme 1. Synthesis of *N*-Alkylated Tacrine Analogues (Figure 6, Target **A**)[a]

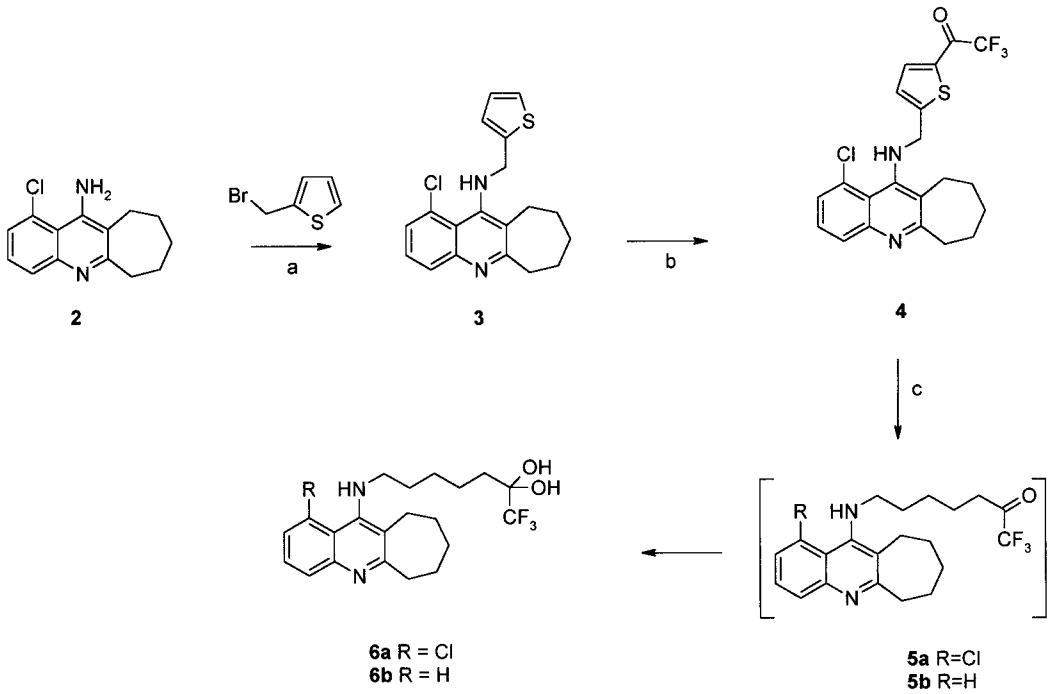

[a] Reagents: (a) (i) NaH, DMF, 50 °C, 1 h, (ii) 2-bromomethylthiophene, 60 °C, 2 h; (b) (i) LDA, THF, −78 °C, 1.5 h, (ii) *N*-methyl-*N*-methoxytrifluoroacetamide, −78 to 0 °C, 0.5 h; (c) Raney Ni, THF, 4.5 h.

(bromomethyl)thiophene gave the *N*-substituted tacrine **3**. This compound was trifluoroacetylated with *N*-methyl-*N*-methoxytrifluoroacetamide to give **4**, which was hydrogenated to give the desired trifluoromethyl ketone **5a** together with the dechlorinated derivative **5b**. On exposure to atmospheric moisture these materials were rapidly converted to their hydrates **6a** and **6b**, which were then separated chromatographically. Previous studies have shown that although alkyl trifluoromethyl ketones readily hydrate to form geminal diols they are in equilibrium, in solution, with sufficient ketone to act as potent serine hydrolase inhibitors.[40]

The aminoquinoline targets **B** and **C** required a different synthetic approach. By reacting the requisite aminobenzonitrile **7a**−**c** with a β-keto ester, using well-known Lewis acid-mediated cyclization conditions,[41] the aminoquinolines **8a**−**c** were efficiently formed (Scheme 2). They were then reduced to **9a**−**c** and chlorinated to give **10a**−**c**. These chloromethyl intermediates were reacted with phthalimide to give, after hydrazine cleavage, the amines **11a** and **11b**. Alkylation of these amines proved unsuccessful, using a variety of standard conditions. An alternative approach, as outlined in Scheme 2, relied upon the generation of a trifluoromethylated lactone **12**, a derivative of succinic anhydride, by reaction with Rupert's reagent.[42] While purification of **12** proved troublesome, the crude material could be reacted directly with amines **11a** and **11b**. Analysis of the resulting products revealed them to be the lactones **13a** and **13b**, rather than the desired open chain target amides of type **B**.

The thiol **14**, required for the S-linked target **C**, was made by reaction of **10a** with thiourea, followed by base hydrolysis (Scheme 3). The 5-bromo-1,1,1-trifluoro-2-pentanone (**16)** was obtained in two stages from butyrolactone via **15**.[42] Alkylation of **14** with **16** unexpectedly gave only the substituted tetrahydrofuran **17**. This, presumably, resulted from preferential attack of the thiolate of **14** on the ketone, followed by cyclodebromination.

We set out to make the final set of targets, the substituted aminoquinolines **D**, from aminoquinoline alcohol intermediates **9a**−**c**. However, alkylation with benzyl bromides proved ineffective; little reaction occurred under standard basic or phase-transfer conditions. However, benzyl ethers, such as **18**, could be made from the chloromethylaminoquinoline **10a** by reaction with excess benzyl alcohols at high temperature (Scheme 4). The key trifluoroacetylbenzyl alcohol **22** was obtained from the 3-bromobenzyl alcohol (**19**), and this similarly yielded the target compounds **23a**−**c** with **10a**−**c**.

The inaccessibility of the required benzyl thiols dictated a different approach for the corresponding sulfur-linked analogues, shown in Scheme 5. 3-Trifluoroacetylbenzyl bromide (**26)** was made in two straightforward stages from 3-bromotoluene (**24)**. The thiol **14** was deprotonated with sodium hydride, and the resultant thiolate reacted, on heating with excess benzyl bromides such as **26**, to afford thioethers. Thus, the type **D** target aminoquinoline **27** was made, together with other analogues, such as related ketone **29**. **27** was subsequently reduced with sodium borohydride to afford the trifluoromethyl alcohol **28**.

In contrast to aliphatic trifluoromethyl ketone examples, the aryl trifluoromethyl ketones **23a**−**c** and **27** were less susceptible to hydration and were isolated in the ketone forms, from chloroform. Although they hydrated substantially in water, a significant proportion of the keto form was maintained. The unfluorinated ketone **29** showed no tendency to hydrate.

Scheme 2. Synthesis of *N*-Alkylated Aminoquinolines (Figure 6, Target **B**)[a]

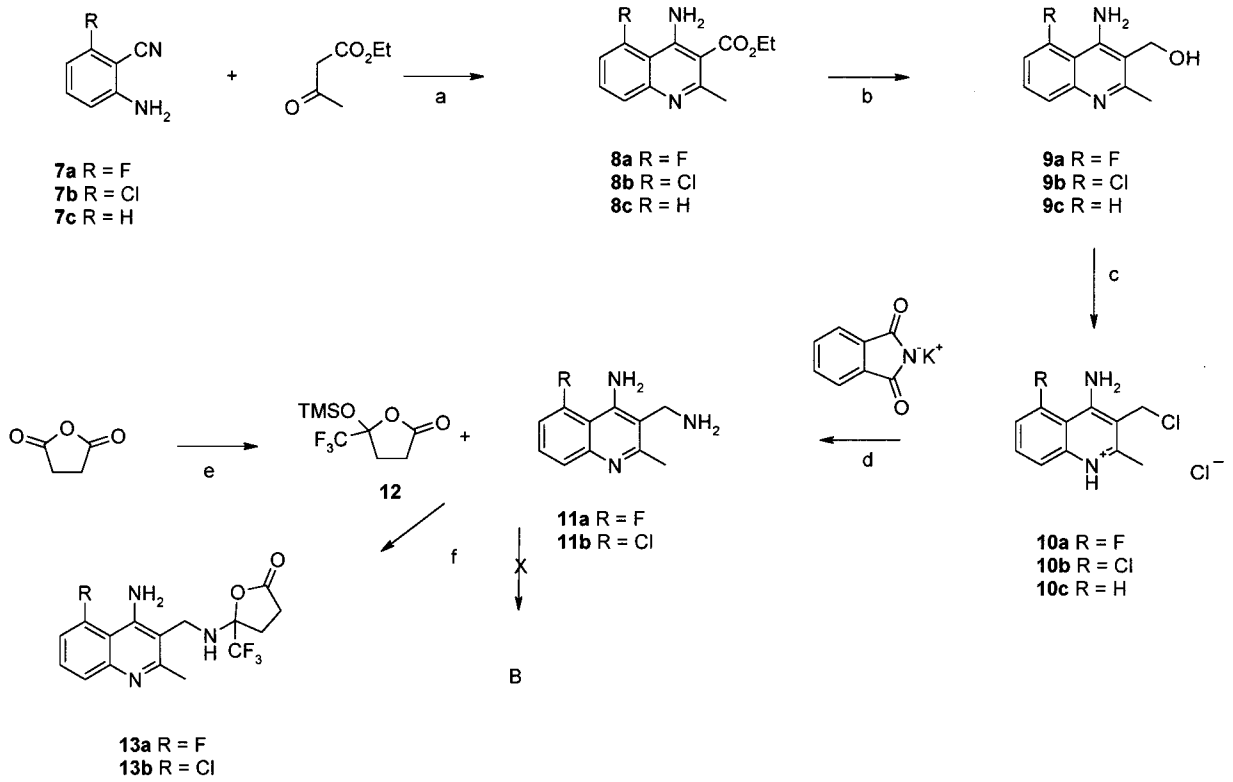

[a] Reagents: (a) (i) $SnCl_4$, PhMe, room temperature to reflux, 5 h, (ii) NaOH, 0−5 °C, 0.5 h; (b) $LiAlH_4$, THF, 4 h; (c) $SOCl_2$, reflux, 1 h; (d) (i) potasium phthalimide, dioxane, (ii) $NH_2NH_2{\cdot}H_2O$, dioxane; (e) CF_3TMS; (f) TBAF.

Scheme 3. Synthesis of *S*-Alkylated Aminoquinolines (Figure 6, Target **C**)[a]

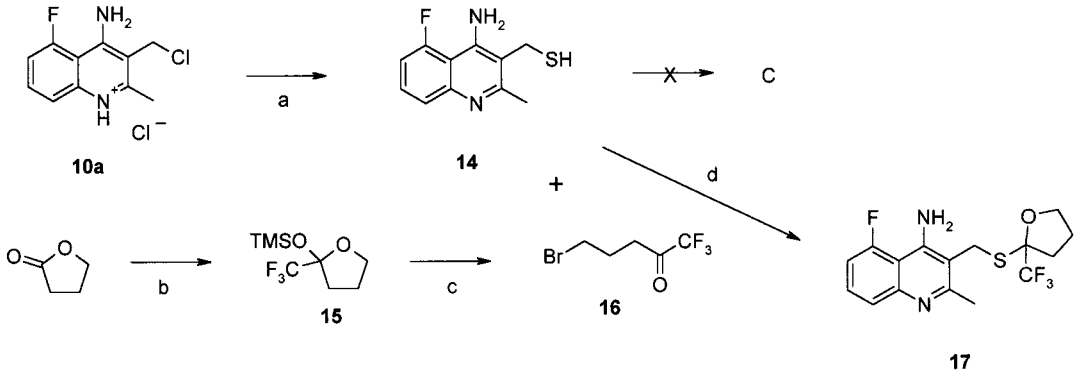

[a] Reagents: (a) (i) thiourea, DMF, 100 °C, 2 h, (ii) NaOH, reflux, 2 h; (b) CF_3TMS; (c) concentrated HBr; (d) (i) NaH, DMF, room temperature to 50 °C, 0.5 h, (ii) **15** added at room temperature, heat 60 °C, 2 h.

Structure−Activity Relationships

Some key intermediates and all final products of the synthetic sequences described above were tested on *Torpedo* AChE for inhibitory activity (Table 1).

The tacrine analogue **2** was chosen as a starting point for the synthesis of target **A** because it contains both the seemingly favored halogen substituent and the fused seven-membered ring.[38,39] The activities of compounds **6a** and **6b**, which conform to this target, compare well with those of tacrine and **2**. The IC_{50} of the more rigid intermediate **4** is in the same range of activity, although modeling had suggested that it would fit the active site less well. The poorer fit to the active site may be offset by the entropic benefit of greater rigidity. In comparison with **3**, the trifluoroacetyl group of **4** dramatically enhances activity, by about 60-fold, which is consistent with the anticipated direct interaction of this group with the enzyme. However, since none of the inhibitors of type **A** was more active than the starting point **2**, we moved onto derivatives of aminoquinolines (targets **B**, **C**, and **D**).

Simple 4-aminoquinolines are relatively poor inhibitors compared to tacrine, and this activity is not significantly enhanced by the introduction of functional side chains, such as those present in the intermediate **8a**, **9a**, or **11a** (i.e., carboxyl ester, OH, NH_2). These compounds tend to have IC_{50} values in the micromolar range, as do the more functional unexpected products **13a,b** and **17**.

Unlike the simpler aminoquinolines, the target **D** compounds **23a**−**c** and **27** are very potent, all showing IC_{50} values in the low nanomolar range. The nature of

Scheme 4. Synthesis of 3-Benzyloxyaminoquinolines (Figure 6, Target **D**)[a]

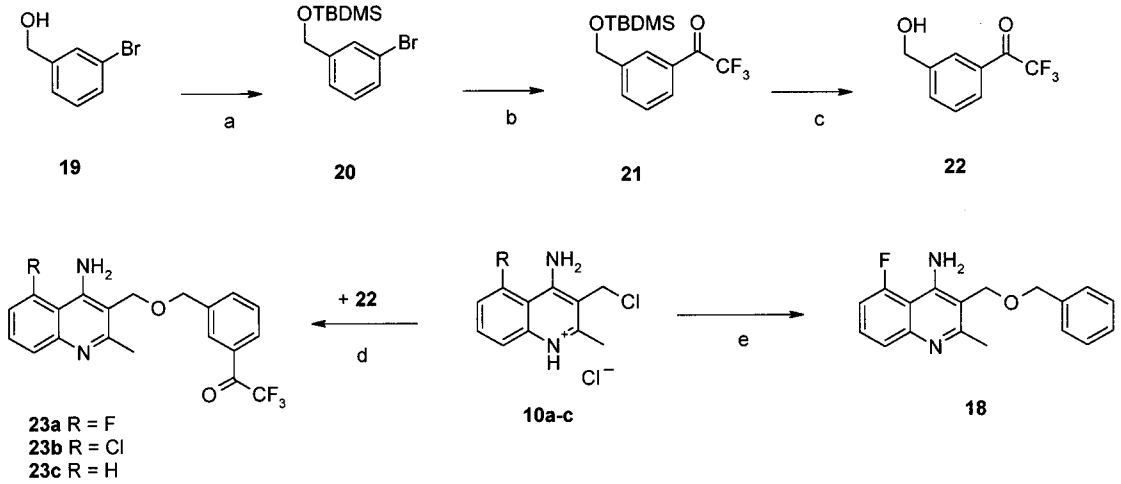

[a] Reagents: (a) TBDMSCl, imidazole, DMF; (b) (i) BuLi, Et_2O, 0 °C, (ii) *N*-trifluoroacetylpiperidine, 0 °C to room temperature, 0.5 h; (c) HCl/MeOH; (d) excess **22**, 120 °C, 4 h; (e) excess benzyl alcohol, **10a**, 120 °C, 4 h.

Scheme 5. Synthesis of 3-Benzylthioaminoquinolines (Figure 6, Target **D**)[a]

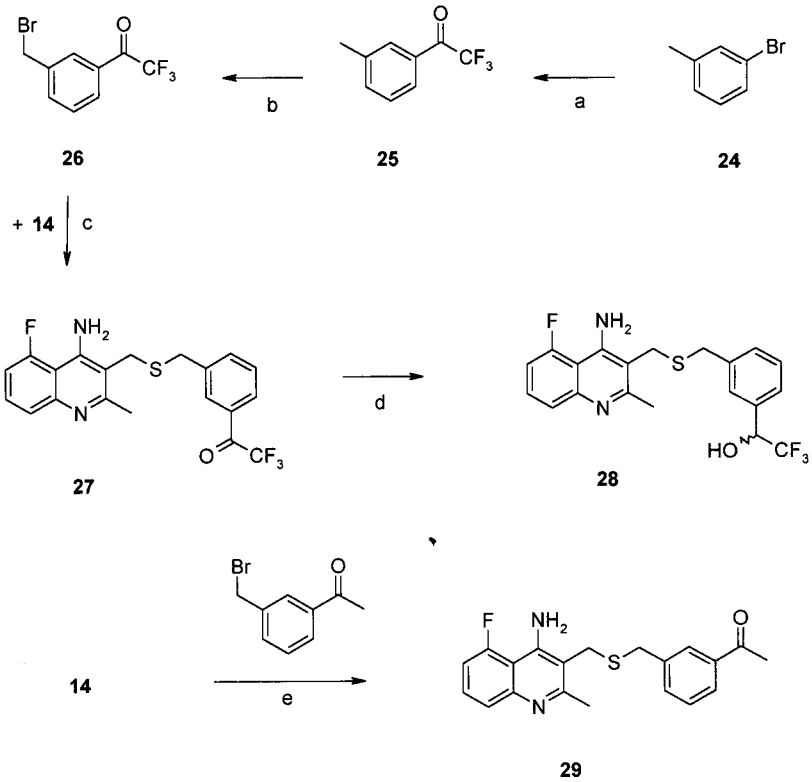

[a] Reagents: (a) (i) Mg, Et_2O, reflux, (ii) trifluoroacetic acid, reflux; (b) NBS, CCl_4, reflux, 3 h; (c) (i) **14**, NaH, DMF, 60 °C, 1 h, (ii) **26**, 60 °C, 2 h; (d) $NaBH_4$, THF, room temperature, 1 h; (e) **14**, NaH, DMF, 60 °C, 1 h, (ii) benzyl bromide, 60 °C, 2 h.

the heteroatom linking group makes no difference to the activity (**23a** versus **27**) and neither does the nature of the atom at the 5-position (F, Cl, or H, for **23a**−**c**).

Close analogues that lack the full trifluoromethyl ketone moiety (**18**), or have been reduced to the secondary alcohol **28**, or those that contain hydrogen atoms instead of fluorines (**29**) are, respectively, 500-, 3700-, and 5000-fold less active than their parent compound. These observations are consistent with the type **D** target compounds interacting, as we postulated, with the active site serine 200 to form a transition-state analogue, of the sort shown in Figure 3. Indeed, although the secondary alcohol **28** could occupy both the oxyanion hole and methyl binding pockets, it is incapable of forming a covalent bond to serine 200, while the unfluorinated ketone **29** is, presumably, insufficiently reactive to act as a nucleophilic trap for the serine.

The study of compounds **18**, **28**, and **29** as well as the intermediates **8a**, **9a**, and **11a** thus showed the importance of the $COCF_3$ group as a key moiety in the design of our inhibitors.

However, the potent activity of **23a**−**c** and **27** is not only due to the trifluoromethyl ketone as compound **26**, which lacks the aminoquinoline moiety, is 100-fold less active than **23a**−**c** and **27**.

Table 1. In Vitro IC_{50} Values for the Inhibition of *Torpedo* AChE

compd no.	IC_{50} (nM)	structure in	compd no.	IC_{50} (nM)	structure in
tacrine	8.2	Figure 1	**13b**	7.2×10^3	Scheme 2
2	2.4	Scheme 1	**17**	18×10^3	Scheme 3
3	740	Scheme 1	**18**	2.0×10^3	Scheme 4
4	12	Scheme 1	**23a**	3.8	Scheme 4
6a	36	Scheme 1	**23b**	5.1	Scheme 4
6b	14	Scheme 1	**23c**	3.0	Scheme 4
8a	2.6×10^3	Scheme 2	**26**	360	Scheme 5
9a	2.6×10^3	Scheme 2	**27**	3.0	Scheme 5
11a	19×10^3	Scheme 2	**28**	11×10^3	Scheme 5
13a	14×10^3	Scheme 2	**29**	15×10^3	Scheme 5

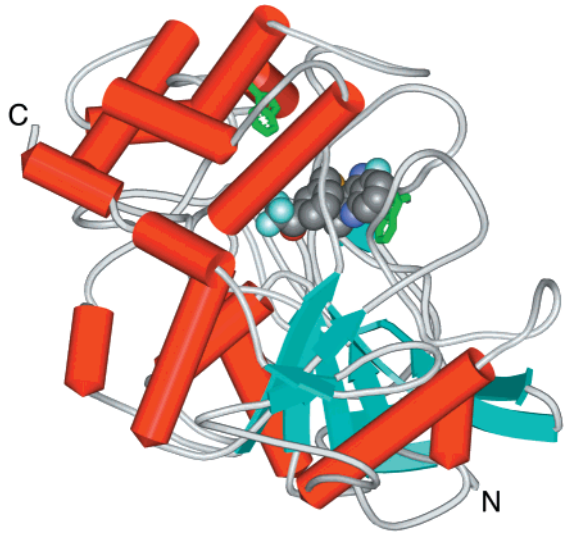

Figure 7. Schematic representation of binding of **27** to TcAChE. The secondary structure of the enzyme is rendered as red cylinders for helices, cyan arrows for sheet structures, and gray tubing for the random coil. The bound inhibitor is shown as solid spheres (carbon in gray, nitrogen in blue, oxygen in red, and fluorine in light blue). Trp84 is shown in green tubing partially hidden by the inhibitor, and Trp279, which marks the entrance to the gorge, is shown as green tubing near the top/center of the picture.

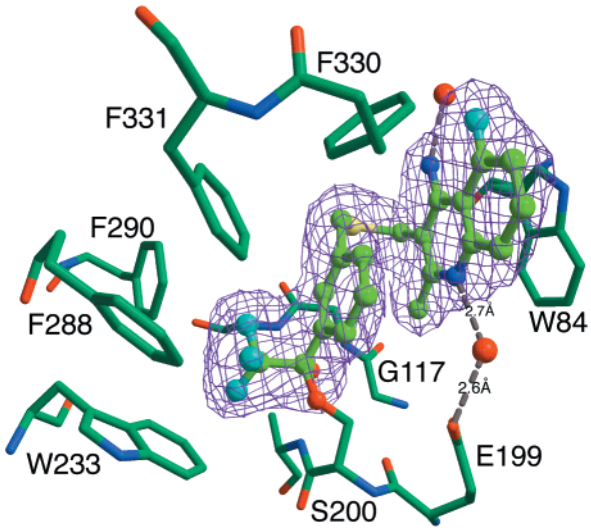

Figure 8. Simulated annealing omit map for the inhibitor 27 contoured at 4σ (purple density), calculated by CNS. The protein residues are rendered as dark green stick models, and the inhibitor is rendered as a light green ball stick model. Carbon atoms are colored green, oxygen red, nitrogen dark blue, and fluorine cyan. Gly118, Gly119, and Ala201, whose nitrogen atoms make up the oxyanion hole, are not labeled for clarity. Two key water molecules are shown as red spheres. The contact between the amine nitrogen of the inhibitor and a water molecule shown partialy behind the electron density is 2.8 Å long. The orientation is similar to that shown in Figure 7. The picture was made with XtalView/Raster3D.[51,52]

We have therefore achieved the synergistic effect of the aminoquinoline group and the $COCF_3$ moiety that was aimed for in this work.

Comparison of the Anticipated Binding Mode with That Experimentally Observed

Ultimately, the extent to which structure-based design is successful depends on our ability to predict protein−ligand interactions. To assess the method used here, we thus solved the crystal structure of compound **27** complexed with *T. californica* AChE as described in the Experimental Section. Figure 7 shows an overall view of the complex while Figure 8 shows the simulated annealing omit map for the inhibitor **27**. As is detailed below, there are both similarities and differences between the predicted and observed binding modes (Figure 9).

The position of the trifluoroacetyl group was predicted well, which is perhaps not surprising because this is constrained by a covalent bond to the protein.

The largest difference, however, occurs for the 4-aminoquinoline bicycle, which is flipped over in the predicted structure with respect to the observed structure. Although at first sight this appears to be a major change, the flip largely preserves the position of the aminopyridine ring (allowing a similar hydrogen-bonding pattern) and also preserves the stacking interaction of the bicycle with Trp84. The origin of the flip comes from the template on which the design work was carried out: the tacrine had been incorrectly modeled into the active site in a flipped orientation (see the Computational Methods).

The conformation of the linker group was poorly predicted, and this may in part be due to the unusual conformation of this in the observed structure, which has an eclipsed torsion in one of the C−S bonds. The conformation of the linker group allows an intramolecular stacking interaction to occur between the phenyl ring and the 4-aminoquinoline, which was not predicted in the modeled structure, and probably offsets the penalty of the eclipsed bond.

Despite the differences between the predicted and observed binding modes, the design strategy was successful. Molecule **27** is a potent inhibitor with an IC_{50} value of 3 nM. Although the predicted binding was wrong in some matters of detail, **27** does span the trifluoroacetyl and tacrine binding sites that were targeted at the outset.

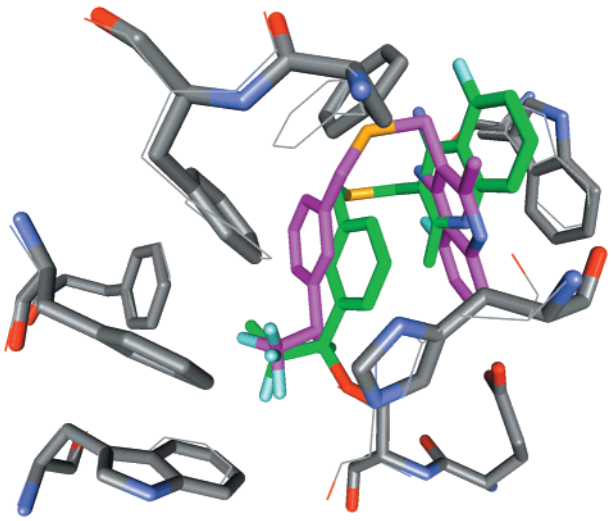

Figure 9. Comparison of the crystallographically observed binding of 27 (green carbon atoms) with the predicted binding mode (magenta carbons). The wire-frame protein atoms relate to the predicted structure. The orientation is similar to that shown in Figure 7.

Conclusions

On the basis of the structures of enzyme−inhibitor complexes, we have designed novel and potent reversible inhibitors targeting AChE from *T. californica* which occupy most of the functional region of the active site. The modeled complex of one of these inhibitors has been compared to the structure obtained by X-ray crystallography, and despite some differences between the predicted and observed complexes, the design strategy can be argued to have been successful. Although it is difficult to predict exact binding modes with the current technologies, they provide us with approximate models that are often good enough to allow the design of active molecules.

The type **D** inhibitors, which present a good inhibitory efficiency and a limited conformational flexibility, provided us with an ideal template, and starting point for further synthesis. This has allowed us to improve the potency of the inhibitors as well as to explore species differences between AChEs, the design of insect-selective active site AChE inhibitors being of particular interest to us. This work has been guided by the crystallographic studies and will be reported elsewhere.

In a contemporaneous study to the work described in this paper, researchers at the Universitat de Barcelona have developed other potent AChE inhibitors using a similar hybridization strategy, but instead combining the features of tacrine with those of huperzine A.[27,29,43−45] The success of both their work and ours indicates the utility of hybridization strategies in structure-based ligand design programs.

Experimental Section

Computational Methods. Details of the template definition are as follows. The aminoquinoline ring was positioned as closely as possible to the tacrine location inferred from preliminary crystallographic results, which had been made available to the modeling group in advance of the full 3D coordinates. The ring nitrogen was within H-bonding distance of the His440 backbone carbonyl oxygen. When the fully refined 3D coordinates of the tacrine complex became available, we realized that the docked aminoquinoline was flipped over relative to tacrine. The two aminopyridine rings were in much the same position, but the second ring of the aminoquinoline was near the saturated ring of tacrine rather than the unsaturated ring it more closely resembled.

The trifluoroacetyl group was located in the same position as the acetyl group of acetylcholine as modeled into the structure of the apoenzyme by Sussman et al. (1ACE). The resulting template was characterized by the distances in Figure 5.

The conformational searching was carried out with the systematic search option of SYBYL (version 6.01, Tripos Inc., 1699 South Hanley Rd., St. Louis, MO, 63144). This was used to generate all conformations of the flexible linking chain of each candidate molecule, such that the distance constraints were met to within a predefined tolerance. Depending on the molecule, tolerances of between ±0.3 and ±1.0 Å were used; torsion increments were 5°, and the van der Waals reduction factor was 0.85. An in-house program (CONPICKS) was used to select up to 200 representative conformations from the search output for each molecule. Each conformation was energy minimized with the molecular mechanics program AESOP (B. B. Masek, unpublished results), but with the nine distances constrained to stay near their template values. The strain energy of each conformation relative to the global minimum was estimated, and conformations with strain energies >10 kcal/mol were rejected. The surviving, unique conformations were overlaid on the template and inspected in the active site. Molecules were qualitatively assessed by visual inspection, on the basis of their goodness of fit to the template, steric clashes with the protein, conformational strain, solvent accessibility of H-bonding groups, and number of flexible torsions.

Chemistry. Melting points were determined with a Gallenkamp apparatus and are uncorrected. ^{1}H NMR and ^{19}F NMR spectra (270 MHz) were taken on a JEOL GSX270 spectrometer. Chemical shifts are given in δ values (ppm) with tetramethylsilane (for ^{1}H NMR) and $CFCl_3$ (for ^{19}F NMR) as internal standard. Abbreviations used in the NMR analyses are as follows: br s = broad singlet, d = doublet, m = multiplet, q = quartet, t = triplet. The IR spectra were recorded with a Perkin-Elmer 881 infrared spectrophotomer using neat liquid films (for liquids) or Nujol Mulls (for solids). The HRMS spectra were taken on a Micromass Autospecq spectrometer, the electrospray mass spectra on a Micromass Platform LC spectrometer in electrospray mode, and the autoprobe mass spectra on a Micromass TRIO2000 spectrometer. Where analyses are indicated only by symbols of the elements, the analytical results obtained for those elements (performed by Medac Ltd., Brunel University, U.K.) were within ±0.4% of theoretical values.

General Procedures. 11-Amino-1-chloro-6*H*-cyclohepta[*b*]quinoline (2). $ZnCl_2$ (anhydrous, 45.0 g, 0.33mol) was added to a solution of 2-amino-6-chlorobenzonitrile (50.0 g, 0.33mol) in cycloheptanone (280 mL). The mixture was stirred at 120 °C for 3 h. When a dense precipitate formed, the mixture was cooled to room temperature and the solvent decanted off. The residual solid was triturated with EtOAc (150 mL) and filtered off. This was added to 2 M NaOH (400 mL) and stirred for 1.5 h. CH_2Cl_2 (500 mL) was then added and stirring continued for 0.5 h. Undissolved solid was filtered off. The organic phase of the filtrate was washed with water, dried ($MgSO_4$), and evaporated to give the crude product. Recrystallization from CH_2Cl_2/EtOAc gave the product as a white solid (55.3 g, 68%): mp 195−196 °C; ^{1}H NMR ($CDCl_3$) δ 1.60−1.95 (6H, m), 2.67−2.72 (2H, m), 3.05−3.12 (2H, m), 5.82 (1H, br s), 7.30−7.42 (2H, m), 7.75 (1H, m). Anal. (C_{14} $H_{15}ClN_2$) C, H, N.

1-Chloro-11-(2-Thiophenylmethyl)amino-6*H*-cyclohepta[*b*]quinoline (3). NaH (60% in oil, 2.30 g, 0.0575mol) was suspended in dry DMF (150 mL), and compound **2** (13.20 g, 0.054mol) in dry DMF (150 mL) was added at 20 °C with stirring over 0.5 h. When effervescence had subsided, the mixture was heated at 50 °C for 1 h and then cooled to room temperature. A solution of 2-bromomethylthiophene (9.50 g,

0.054mol) in dry DMF (50 mL) was added, and the mixture was heated at 60 °C for 2 h, then cooled to room temperature, and poured into water. The mixture was adjusted to pH 12 with 2 M NaOH and extracted three times with CH_2Cl_2. The organic extracts were combined, washed with water, dried ($MgSO_4$), and evaporated to give crude **3**. This was purified by chromatography on silica using $CHCl_3$/EtOAc (80:20), giving the product as a pale brown solid (9.8 g, 53%): mp 105−106 °C; ^{1}H NMR ($CDCl_3$) δ 1.70−2.00 (6H, m), 3.00−3.10 (2H, m), 3.10−3.20 (2H, m), 4.45 (2H, d), 5.95 (1H, br t), 6.95−7.02 (2H, m), 7.20−7.27 (1H, m), 7.37−7.47 (2H, m), 7.85−7.92 (1H, m). Anal. ($C_{19}H_{19}ClN_2S$) C, H, N.

1-Chloro-11-(2-Trifluoroacetyl-5-thiophenylmethyl)-aminocyclohepta[*b*]quinoline (4). Diisopropylamine (0.59 g, 0.0058 mol) was dissolved in dry THF (20 mL) and *n*-butyllithium (3.65 mL of a 1.6 M solution in hexane, 0.0058 mol) added dropwise, under nitrogen with stirring at −65 °C. The solution was then stirred at this temperature for 10 min. A solution of compound **3** (1.00 g, 0.0052 mol) in dry THF (15 mL) was added dropwise at −65 °C and stirred at this temperature for 1.5 h. A solution of *N*-methyl-*N*-methoxytrifluoroacetamide in THF (5 mL) was added and the reaction allowed to warm to 0 °C and maintained at this temperature for 0.5 h. It was then allowed to warm to room temperature, poured into cold water, made alkaline with 2 M NaOH, and extracted three times with CH_2Cl_2. The organic extracts were combined and washed with water, dried ($MgSO_4$), and evaporated to give the crude product which was purified by chromatography on silica using $CHCl_3$/EtOAc (85:15) to give **4** as a pale yellow solid (0.43 g, 34%): mp 105−106 °C; ^{1}H NMR ($CDCl_3$) δ 1.75−1.91 (6H, m), 3.04−3.08 (2H, m), 3.16−3.20 (2H, m), 4.48 (2H, d, J = 6.5), 5.97 (1H, br), 7.15 (1H, J = 4.2), 7.44−7.46 (2H, m), 7.87−7.93 (2H, m); ^{19}F NMR ($CDCl_3$) −72.6 ppm; MH^+ (electrospray) 438 (1 Cl); IR (solid) 1684 cm^{-1}; Anal. ($C_{21}H_{18}ClF_3N_2OS\cdot 0.25H_2O$) H, N, C calcd 57.47, found 56.88.

1-Chloro-11-(6,6-Dihydroxy-7,7,7-trifluoroheptan-1-yl)-aminocyclohepta[*b*]quinoline (6a) and 11-(6,6-Dihydroxy-7,7,7-trifluoroheptan-1-yl)aminocyclohepta-[*b*]quinoline (6b). Compound **4** (0.900 g, 0.00205mol) was dissolved in THF at 20 °C and Raney nickel added (7.0 mL of 50% suspension, excess). At 1.5 h intervals more Raney nickel was added (15 mL in three portions). After 4.5 h total the mixture was filtered through Celite and the precipitate washed with a mixture of THF/water (3:1, 50 mL). The filtrate was evaporated under reduced pressure, and the residue was purified by chromatography on silica gel using methanol/chloroform (8:92), giving a mixture of **6a** and **6b**. These were separated by chromatography on silica gel using dichloromethane/hexane/triethylamine (80:20:2) to give 0.17 g (15%) of **6a** and 0.21 g (26%) of **6b** as yellow oils. Data for compound **6a**: ^{1}H NMR ($CDCl_3$) δ 1.36−1.97 (14H, m), 2.65−2.80 (2H, m), 2.90−3.0 (2H, m), 3.05−3.15 (4H, m), 5.30 (1H, br), 7.35−7.45 (2H, m), 7.80−7.90 (1H, m); ^{19}F NMR (CD_3OD) −83.0 ppm; MH^+ (electrospray) 432 (1 Cl). Anal. ($C_{21}H_{26}ClF_3N_2O_2$) H, N, C calcd 58.54, found 57.18. Data for compound **6b**: ^{1}H NMR ($CDCl_3$) δ 1.35−1.90 (14H, m), 2.65−2.75 (2H, m), 2.85−2.95 (2H, m), 3.15−3.36 (4H, m), 3.50 (1H, br), 7.37−7.47 (1H, m), 7.52−7.60 (1H, m), 7.80−7.90 (1H, m), 7.90−8.00 (1H, m); ^{19}F NMR (CD_3OD) −83.1 ppm; MH^+ (electrospray) 397. Anal. ($C_{21}H_{27}F_3N_2O_2$) H, N, C calcd 63.62, found 62.10.

4-Amino-3-carboxyethyl-5-fluoro-2-methylquinoline (8a). Ethyl acetoacetate (36.8 g, 0.28 mol) was added to a solution of **7a** (38.5 g, 0.28 mol) in toluene (800 mL). Stannic chloride (147.5 g, 0.57 mol) was then added in a slow stream to the stirred mixture while the temperature was kept within the range 20−40 °C by external cooling using an ice/water bath. The resultant mixture was cautiously heated to initiate an exothermic reaction which was thereafter moderated by external cooling with an ice bath. The mixture was then stirred under reflux for 5 h and cooled to room temperature and the supernatant liquid decanted from an oily residue. The residue was triturated with EtOAc (750 mL) and a yellow solid filtered off. This was added to sodium hydroxide solution (2 M) and stirred at 0−5 °C for 0.5 h, and the resulting mixture was extracted with EtOAc (3 × 250 mL). The extracts were combined, washed with water, dried ($MgSO_4$), and evaporated to give a yellow crystalline solid (54.5 g, 78%): mp 70−71 °C; ^{1}H NMR ($CDCl_3$) δ 7.66 (2H, br s), 7.62 (1H, m), 7.55 (1H, m), 7.00 (1H, m), 2.77 (3H, s), 4.42 (2H, q), 1.44 (3H, t). Anal. ($C_{13}H_{13}FN_2O_2$) C, H, N.

4-Amino-3-carboxyethyl-5-chloro-2-methylquinoline (8b). 8b was obtained from **7b** and purified by chromatography on silica using $CHCl_3$/MeOH (98:2) (75%). An analytical sample was recrystallized from hexane: mp 70 °C; ^{1}H NMR ($CDCl_3$) δ 8.25 (2H, br s), 7.30−7.77 (3H, m), 4.40 (2H, q), 2.74 (3H, s), 1.42 (3H, t); M^+ (probe) 264 (1 Cl). Anal. $C_{13}H_{13}ClN_2O_2$) C, H, N.

4-Amino-3-carboxyethyl-2-methylquinoline (8c). 8c was obtained from **7c** (72%). An analytical sample was recrystallized from hexane: mp 137 °C; ^{1}H NMR ($CDCl_3$) δ 7.32−7.88 (4H, m), 7.05 (2H, br s), 4.41 (2H, q), 2.80 (3H, s), 1.45 (3H, t). Anal. ($C_{13}H_{14}N_2O_2$) C, H, N.

4-Amino-5-fluoro-3-hydroxymethyl-2-methylquinoline (9a). Lithium aluminum hydride (9.9 g, 0.26 mol) was mixed with THF (1.2 L), and a solution of compound **8a** (54.5 g, 0.22 mol) in THF (0.4L) was added to the stirred mixture, over 1 h at 18−25 °C under a nitrogen atmosphere. After the mixture was stirred for a further 3 h, water (75 mL) was added dropwise with external ice/water cooling. The mixture was then acidified with aqueous hydrochloric acid (2 M, 0.3 L), after which it was made basic with saturated sodium hydroxide solution (100 mL). The organic layer was separated, dried ($MgSO_4$), and evaporated. The residue was recrystallized from ethanol (0.4 L) to give 4-amino-5-fluoro-3-hydroxymethyl-2-methylquinoline as pale yellow crystals (31 g, 68%): mp 218−220 °C; ^{1}H NMR (DMSO) δ 6.69−7.45 (3H, m), 6.25 (2H, br s), 4.95 (1H, t), 4.50 (2H, d), 2.45 (3H, s). Anal. ($C_{11}H_{11}FN_2O$) C, H, N.

4-Amino-5-chloro-3-hydroxymethyl-2-methylquinoline (9b). 9b was obtained from compound **8b** (65%): mp 240−241 °C; ^{1}H NMR (DMSO) δ 7.30−7.70 (3H, m), 6.72 (2H, br s), 5.10 (1H, t), 4.67 (2H, d), 2.57 (3H, s); M^+ (probe) 222 (1 Cl). Anal. ($C_{11}H_{11}ClN_2O$) C, H, N.

4-Amino-3-hydroxymethyl-2-methylquinoline (9c). 9c was obtained from compound **8c** (84%): ^{1}H NMR (DMSO) δ 7.27−8.07 (4H, m), 6.35 (2H, br s), 4.52 (2H, s), 2.40 (3H, s).

4-Amino-3-chloromethyl-5-fluoro-2-methylquinoline Hydrochloride (10a). Compound **9a** (40.0 g, 0.19 mol) was added in portions to stirred thionyl chloride (180 mL) over 5 min (exothermic reaction). The resulting mixture was stirred under reflux for 1 h, after which it was evaporated to leave a residue. The residue was washed with ethanol-free chloroform (75 mL) and the white solid filtered off (49 g, quantitative): ^{1}H NMR (DMSO) δ 2.70 (3H, s), 5.00 (2H, s), 7.35−7.45 (1H, m), 7.80−7.90 (2H, m), 8.50 (2H, br s), 14.90 (1H, s). Anal. ($C_{11}H_{11}Cl_2FN_2$) H, N; C calcd 50.60, found 50.08.

4-Amino-5-chloro-3-chloromethyl-2-methylquinoline Hydrochloride (10b). 10b was obtained from compound **9b** (94%): ^{1}H NMR (DMSO) δ 2.72 (3H, s), 5.00 (2H, s), 7.62−8.10 (3H, m), 8.70 (2H, br s), −13.17 (1H, s).

4-Amino-3-chloro-2-methylquinoline Hydrochloride (10c). 10c was obtained from compound **9c** (88%).

4-Amino-5-fluoro-2-methyl-3-(aminomethyl)quinoline (11a). Compound **10a** (1.20 g, 0.0046 mol) was added to a stirred suspension of potassium phthalimide (2.12 g, 0.0115 mol) in DMF (35 mL) at 100 °C, stirred for 2 h at 100 °C, then cooled, and evaporated. The residue was triturated with water, and the solid was filtered off, washed with 2 M NaOH and then with cold water, and air-dried. This was suspended in refluxing EtOH (30 mL), and hydrazine hydrate (0.60 mL, excess) was added. It was stirred under reflux for 1 h, evaporated, and concentrated. HCl (3 mL) and water (1.2 mL) were then added, and the mixture was stirred under reflux for 1 h, cooled, diluted with water (50 mL), and then made alkaline with 2 M NaOH. It was extracted several times with CH_2Cl_2, and the extracts were dried ($MgSO_4$) and evaporated to give the product as a pale yellow solid (0.28 g, 30%): mp

111−112 °C; ^{1}H NMR ($CDCl_3$) δ 6.90−7.70 (3H, m), 6.50 (2H, br), 4.11 (2H, m), 2.65 (3H, s), 1.40 (2H, br). Anal. ($C_{11}H_{12}FN_3$) C, H, N.

4-Amino-5-chloro-2-methyl-3-(aminomethyl)quinoline (11b). 11b was obtained from **10b** and purified by chromatography using CH_2Cl_2/MeOH/NEt_3 (4:1:0.1) (65%): ^{1}H NMR ($CDCl_3$) δ 7.30−7.75 (3H, m), 7.12 (2H, br-s), 4.08 (2H, s), 2.61 (3H, s), 1.40 (2H, br s); M^+ (probe) 221 (1 Cl).

5-Trifluormethyl-5-trimethylsilyloxy-γ-butyrolactone (12). Trimethylsilyltrifluoromethane (4.81 g, 0.034 mol) was added to a stirred suspension of succinic anhydride (3.38 g, 0.034 mol) in dry THF (20 mL) under dry nitrogen. Tetrabutylammonium fluoride (1.0 M in THF, 0.50 mL, 0.00050 mol) was then added, stirred at 60 °C for 7 h, and evaporated. The residue was distilled (bp 120−130 °C, 15 mmHg), giving a clear colorless oil (2.47 g, 30%). GC/MS analysis showed two peaks of equal intensity both having molecular weight 242. The product was used in the preparation of **13a** and **13b**.

4-Amino-5-fluoro-2-methyl-3-[*N*-(4-trifluoromethyl-γ-butyrolacton-4-yl)]aminomethylquinoline (13a). Compound **12** (0.39 g, 0.0016mol) was added to a stirred suspension of compound **11a** (0.33 g, 0.0016 mol) in dry MeCN (15 mL), and the mixture was stirred under reflux for 8 h and then cooled to room temperature. The crystalline precipitate was filtered off, dissolved in warm MeOH (5 mL), and filtered. The filtrate was evaporated to give the product as a pale yellow solid (0.15 g, 25%): mp 185−186 °C dec; ^{1}H NMR (DMSO) δ 7.92 (1H, br), 7.37−7.47 (2H, m), 6.96−7.06 (1H, m), 4.55 (2H, ABq), 2.60 (3H, s), 2.00−2.50 (4H, m); ^{19}F NMR ($CDCl_3$) −81.5 ppm; MH^+ (electrospray) 358. Anal. ($C_{16}H_{15}N_3F_4O_2$) C, H, N.

4-Amino-5-chloro-2-methyl-3-[N−(4-trifluoromethyl-γ-butyrolacton-4-yl)]aminomethylquinoline (13b). 13b was obtained from compounds **11b** and **12** and purified by chromatography on silica using EtOAc/MeOH (8:2) (50%): mp 179−181 °C dec; ^{1}H NMR ($CDCl_3$) δ 7.20−7.60 (3H, br), 7.20−7.00 (3H, m), 4.65 (2H, ABq), 2.65 (3H, s), 2.20−2.80 (4H, m); ^{19}F NMR (CD_3OD) −83.6 ppm; M^+ (probe) 373 (1 Cl). Anal. ($C_{16}H_{15}F_3ClN_3O_2$) H, N, C calcd 51.42, found 50.91.

4-Amino-5-fluoro-2-methyl-3-(2-mercaptomethyl)quinoline (14). A solution of thiourea (2.63 g, 0.034 mol) in DMF (15 mL) was added to a stirred suspension of compound **16** (9.0 g, 0.034 mol) in DMF (45 mL), and the mixture was stirred at 100 °C for 2 h. The mixture was then evaporated, and the residue was mixed with 2 M NaOH (65 mL) and stirred at reflux under a nitrogen atmosphere for 2 h. The mixture was cooled to room temperature and filtered. The filtrate was cooled in ice, acidified with concentrated HCl, and then neutralized with $NaHCO_3$ solution. The yellow solid was filtered off and washed with cold water (10 mL) (4.7 g, 61%): ^{1}H NMR (D_2O) δ 7.60 (1H, m), 7.27 (1H, m), 7.15 (H, m), 3.65 (2H, s), 2.55 (3H, s).

2-Trifluoromethyl-2-trimethylsilyloxy-tetrahydrofuran (15). γ-Butyrolactone (10.5 g, 0.12 mol) and CF_3TMS (19.3 g, 0.13 mol) were dissolved in dry THF (50 mL), and 1.1 M TBAF in THF (1 mL) was added dropwise, with stirring, at 0 °C and then stirred for 2 h at 20 °C. The solvent was removed at atmospheric pressure and the residue distilled on the water pump. The product was collected at 50−55 °C,12 mmHg, as a clear colorless liquid (14 g, 50%).

1-Bromo-5,5,5-trifluoropentan-4-one (16). **15** (14.0 g, 0.061 mol) and 48% HBr (35 mL) were heated at 115 °C in a sealed glass tube for 90 h, cooled, mixed with water (200 mL), and extracted with CH_2Cl_2 (3 × 30 mL). The extracts were washed successively with water, saturated sodium bisulfite solution, and then water. The product was dried ($MgSO_4$), and the solvent was removed at atmospheric pressure. The residue was distilled on the water pump. The product was collected at 40−50 °C, 12 mmHg, as a clear colorless liquid (8 g, 60%): ^{1}H NMR ($CDCl_3$) δ 3.40 (2H, t), 2.92 (2H, t), 2.15 (2H, m); M^+ 219.

4-Amino-5-fluoro-2-methyl-3-[*S*-(2-trifluoromethyl-tetrahydrofuran-2-yl)thiomethyl]quinoline (17). NaH (80% in oil, 0.135 g, 0.0045 mol) was added to a stirred suspension of compound **14** (1.00 g, 0.0045 mol) in DMF (45 mL), portionwise at 25 °C. This was stirred at 50 °C for 0.5 h and then cooled to 25 °C, **16** (0.98 g, 0.0045 mol) was added and stirred at 25 °C for 1 h and then at 60 °C for 2 h, and the mixture was evaporated. The residue was mixed with water (20 mL) and extracted with Et_2O (3 × 20 mL). Ether extracts were washed with brine (10 mL), dried ($MgSO_4$), and evaporated. The residue was purified by chromatography on silica using EtOAc/hexane/NEt_3 (9:1:0.05), giving **17** as a white solid (0.51 g, 31%): mp 134−135 °C; ^{1}H NMR ($CDCl_3$) δ 7.65 (1H, d, J = 7.4), 7.47 (1H, m), 7.00 (1H, m), 5.75 (2H, br), 4.25 (2H, t, J = 7.0), 4.10 (2H, ABq, J = 52.7, 10.5), 2.68 (3H, s), 2.00−2.50 (6H, m), 1.70 (3H, m); ^{19}F NMR ($CDCl_3$) −77.6 ppm; M^+ (probe) 360. Anal. ($C_{16}H_{16}F_4N_2OS$) C, H, N.

4-Amino-3-benzyloxy-5-fluoro-2-methylquinoline (18). **18** was obtained from **10a** and benzyl alcohol and purified by recrystallization from hexane (62%): mp 114−115 °C; ^{1}HNMR ($CDCl_3$) δ 6.90−7.70 (8H, m), 5.95 (2H, br s), 4.77 (2H, s), 4.55 (2H, s), 2.57 (3H, s); M^+ 296 (probe). Anal. ($C_{18}H_{17}FN_2O$) C, H, N.

1-Bromo-3-(*tert*-butyldimethylsilyloxymethyl)benzene (20). *tert*-Butyldimethylsilyl chloride (44.8 g, 0.30 mol) in DMF (200 mL) was added to a stirred solution of imidazole (47.0 g, 0.69 mol) and **19** (50.0 g, 0.27 mol) in DMF (75 mL) at 20 °C (ice/water bath cooling), stirred at 50 °C for 20 h, and cooled to room temperature, and water was (1.25 L) added. The mixture was extracted with hexane (3 × 375 mL), and the hexane extracts were washed with water (5 × 250 mL), dried ($MgSO_4$), and evaporated to leave a clear colorless oil (74.5 g).

1-Trifluoroacetyl-3-(*tert*-butyldimethylsilyloxymethyl)benzene (21). A 68.4 g (0.23 mol) sample of compound **20** was dissolved in dry Et_2O (700 mL), and *n*-BuLi (100 mL, 2.5 M in hexanes, 0.25 mol) was added over 15 min, under dry N_2, at 0−5 °C. The clear yellow solution was allowed to warm to 10 °C over 30 min and then recooled to 0 °C. A solution of *N*-trifluoroacetylpiperidine (41.2 g, 0.23 mol) in Et_2O (50 mL) was then added over 30 min at 0−5 °C. The cooling bath was removed, and the solution was stirred for 1 h and then recooled to 0 °C. A saturated NH_4Cl solution (250 mL) was then added. The aqueous portion was extracted with Et_2O (75 mL). The combined ether extracts were washed with NH_4Cl solution (4 × 25 mL) and then water (4 × 25 mL), dried ($MgSO_4$) and evaporated, leaving a clear yellow oil (70.0 g).

3-Trifluoroacetylbenzyl Alcohol (22). A 70.0 g (0.22 mol) sample of compound **21** was dissolved in MeOH (600 mL), and concentrated HCl (60 mL) was added at 10−20 °C (ice/water cooling bath). After the mixture was stirred for 30 min, it was concentrated to 450 mL on a water pump at 25 °C. The residue was diluted with Et_2O (2 L), neutralized with a slurry of $NaHCO_3$/water, then washed with water, dried ($MgSO_4$), and evaporated. The residue was purified by chromatography on silica using EtOAc/hexane (3:2), giving **22** as a pale yellow viscous oil (31.7 g, 66% from 3-bromobenzyl alcohol): IR (Nujol mull) 3334, 1719 cm^{-1}; ^{1}H NMR ($CDCl_3$) δ 7.40−8.00 (4H, m), 4.80 (2H, s).

4-Amino-5-fluoro-2-methyl-3-(3-trifluoroacetylbenzyloxymethyl)quinoline (23a). A mixture of compound **22** (31.0 g, excess) and compound **10a** (7.80 g, 0.030 mol) was stirred at 125−130 °C for 4 h, and HCl was evolved. After the mixture was cooled to room temperature, water (250 mL) was added and the mixture extracted with Et_2O (5 × 500 mL). The clear aqueous portion was cooled in ice and made alkaline to pH 10−12 with 2 M NaOH. This was then extracted with CH_2Cl_2 (5 × 100 mL), and the extracts were dried ($MgSO_4$) and evaporated. The residue was purified by chromatography on silica using EtOAc/NEt_3 (10:0.1), giving **23a** as a white powder (5.5 g, 47%): mp 136−137 °C; ^{1}H NMR ($CDCl_3$) δ 6.95−8.07 (7H, m), 5.97 (2H, br), 4.86 (2H, s), 4.62 (2H, s), 2.60 (3H, s); ^{19}F NMR ($CDCl_3$) −71.8 ppm (95%, free ketone) −84.8 ppm (5%, hydrated ketone); M^+ calcd for $C_{20}H_{16}F_4N_2O_2$ 392.114791, found 392.116037. Anal. ($C_{20}H_{16}F_4N_2O_2 \cdot 0.5H_2O$) C, H, N.

4-Amino-5-chloro-2-methyl-3-(3-trifluoroacetylbenzyloxymethyl)quinoline (23b). **23b** was obtained from com-

Table 2. Data Collection and Processing Statistics

oscillation angle (deg)	0.25					
total number of frames	251					
total number of reflections	409141					
resolution range (Å)	302.5					
number of unique reflections	34411					
redundancy	0	1	2	3	4	>5
% reflections	1.3	6.0	13.1	23.9	30.5	24.1
average redundancy (weighted)	3.5					
overall completeness (%)	98.4					
completeness in highest resolution shell (%)	91.8					

Table 3. Refinement Results

resolution range (Å)	30.0−2.5	R_{work} (%)	18.3
number of protein atoms	4244	R_{free} (5% of reflections) (%)	21.4
number of nonprotein atoms		rms bond deviations (Å)	0.021
solvent (water, PEG, MES)	171, 13, 12	rms angle deviations (deg)	2.0
carbohydrate atoms	42		
inhibitor	28		

pounds **10b** and **22** and purified by chromatography on silica using CH_2Cl_2/MeOH/NEt_3 (96:2:2) (64%): mp 106−107 °C; ^{1}H NMR (DMSO) δ 7.27−7.65 (7H, m), 6.72 (2H, br), 4.65 (2H, s), 4.55 (2H, s), 2.45 (3H, s); ^{19}F NMR (DMSO) −71.0 ppm (11% free ketone) −83.2 ppm (89% hydrated ketone); MH^+ 409 (1 Cl, electrospray). Anal. ($C_{20}H_{16}ClF_3N_2O_2 \cdot H_2O$) C, H, N.

4-Amino-2-methyl-3-(3-trifluoroacetylbenzyloxymethyl)quinoline (23c). **23c** was obtained from compounds **10c** and **22** and purified by chromatography on silica using EtOAc/NEt_3 (99:1) (35%): mp 100−102 °C; ^{1}H NMR ($CDCl_3$) δ 7.40−8.10 (8H, m), 5.40 (2H, br), 4.90 (2H, s), 4.61 (2H, s), 2.67 (3H, s); ^{19}F NMR ($CDCl_3$) −71.9 ppm (99%, free ketone) −78.9 ppm (1%, hydrated ketone); M^+ calcd for $C_{20}H_{17}F_3N_2O_2$ 374.124213, found 374.124035. Anal. ($C_{20}H_{17}F_3N_2O_2 \cdot 0.5H_2O$) H, N; C calcd 62.65, found 62.11.

3-Trifluoroacetyltoluene (25). To a suspension of Mg (9.5 g, 0.39 mol) and I_2 (1 crystal) in dry Et_2O (50 mL) was added 3-bromotoluene (44.5 g, 0.26 mol) with stirring, under N_2, over 0.5 h. The mixture was refluxed for 1 h, diluted with Et_2O (250 mL), and a solution of CF_3CO_2H (10.0 g, 0.39 mol) in Et_2O (100 mL) was added at 10−20 °C with ice/water cooling over 1 h. It was stirred under reflux for 2 h, cooled in ice, poured onto a mixture of ice (500 g), and concentrated HCl (100 mL). The ether layer was separated, washed with saturated $NaHCO_3$ solution (2 • 50 mL), dried ($MgSO_4$), and evaporated. The residue was distilled on a water pump, giving a clear colorless liquid (12.8 g, 77%): bp 65−68 °C, 12 mmHg; ^{1}H NMR ($CDCl_3$) δ 7.80−7.37 (4H, m), 2.40 (3H, s); IR 1719 cm^{-1}.

3-Trifluoroacetylbenzyl bromide (26). To a solution of compound **25** (12.2 g, 0.064 mol) in CCl_4 (110 mL) were added NBS (12.7 g, 0.071 mol) and benzoyl peroxide. The mixture was stirred under reflux under N_2 for 5 h, cooled, and filtered. The filtrate was evaporated, and the residue was dissolved in Et_2O (75 mL), washed with saturated $NaHCO_3$ (25 mL), dried ($MgSO_4$), and evaporated. The residue was then distilled on an oil pump, collecting the product as a pale brown oil (9.4 g, 55%): bp 48−60 °C, 0.2 mmHg; ^{1}H NMR ($CDCl_3$) δ 7.55−8.10 (4H, m), 4.52 (2H, s).

4-Amino-5-fluoro-2-methyl-3-(3-trifluoroacetylbenzylthiomethyl)quinoline (27). Compound **14** (2.00 g, 0.0090 mol) in DMF (50 mL) was stirred at room temperature, and NaH (0.27 g, 80% in oil, 0.0090 mol) was added portionwise. The mixture was stirred at room temperature for 10 min and then at 50 °C for 0.5 h. The mixture was cooled to room temperature, and **26** (2.40 g, 0.0090 mol) was added. The mixture was stirred at 60 °C for 2 h and then evaporated. The residue was mixed with water (50 mL) and extracted with CH_2Cl_2 (2 × 50 mL). The extracts were combined, dried ($MgSO_4$), and evaporated to leave a residue which was purified by chromatography on silica using EtOAc/NEt_3 (10:0.05), giving **27** as a yellow solid (1.00 g, 27%): mp 131−132 °C; ^{1}H NMR ($CDCl_3$) δ 6.90−8.10 (7H, m), 5.57 (2H, br), 3.80 (2H, s), 3.85 (2H, s), 2.54 (3H, s); ^{19}F NMR ($CDCl_3$) −72.7 ppm (95%, free ketone) −85.7 ppm (5%, hydrated ketone); M^+ calcd for $C_{20}H_{16}F_4N_2OS$ 408.091948, found 408.092201. Anal. ($C_{20}H_{16}F_4N_2OS \cdot 0.5H_2O$) C, H, N.

4-Amino-5-fluoro-2-methyl-3-[3-(1,1-dihyroxy-2,2,2-trifluoroethyl)-benzylthiomethyl]quinoline (28). A solution of $NaBH_4$ (0.15 g, 0.000395 mol) in EtOH (3 mL) was added to a stirred solution of compound **27** in EtOH (2.8 mL). The mixture was stirred at room temperature for 18 h and then evaporated. The residue was mixed with water (0.25 mL) and CH_2Cl_2 (5 mL). The CH_2Cl_2 extract was dried ($MgSO_4$) and evaporated, giving **28** as a white solid (0.083 g, 82%): mp 188−189°; ^{1}H NMR (DMSO) δ 6.77−7.47 (7H, m), 6.30 (2H, br), 5.10 (1H, m), 3.85 (2H, s), 3.75 (2H, s), 2.30 (3H, s); ^{19}F NMR (DMSO) −77.01 ppm, −77.04 ppm (1:1, CF_3CH). Anal. ($C_{20}H_{18}F_4N_2OS$) C, H, N.

4-Amino-5-fluoro-2-methyl-3-(3-acetylbenzylthiomethyl)quinoline (29). **29** was obtained from compound **14** and 3-acetylbenzyl bromide and purified by chromatography on silica using CH_2Cl_2/MeOH (97:3) (73%). An analytical sample was prepared by recrystallization from EtOAc: mp 157−158 °C; ^{1}H NMR ($CDCl_3$) δ 6.90−7.95 (7H, m), 5.55 (2H, br), 3.82 (2H, s), 3.75 (2H, s), 2.61 (3H, s), 2.55 (3H, s); M^+ (probe) 354. Anal. ($C_{20}H_{19}FN_2OS$) C, H, N.

Biochemistry. Materials. *T. californica* AChE was purified as described previously.[18,46] Acetylthiocholine iodide (ATCh) and 5,5′-dithiobis(2-nitrobenzoic acid) (DTNB) were purchased from Sigma.

Enzymatic Assays. AChE activity was evaluated spectrophotometrically at 405 nm using the method of Ellman[47] in 0.1 M phosphate buffer, pH 7.8. The enzyme (0.8 μg/L) was incubated for 10 min at room temperature with 10 concentrations of a compound using EtOH as cosolvent (maximum 2.5%). The hydrolysis of the substrate was followed for 18 min after addition of ATCh (500 μM) and DTNB (150 μM) and was corrected for spontaneous hydrolysis of the substrate. The activities were then compared to the activity of a control and expressed as a percent of inhibition. Determinations of IC_{50} were made by least-squares fitting of the Hill equation to the percentage inhibition data. The presented values are the average of at least four determinations. Standard errors are less than 30% of the mean IC_{50} values**.**

X-ray Crystallography. Compound **27** was dissolved in methanol to give a 100 mM stock solution. Soaking solutions (10 mM) were prepared by adding the stock solution to a solution containing 0.5 M MES, pH 5.6, and 36% PEG 200 (v/v). A crystal of *Tc*AChE was transferred to an 8 mL drop of the soaking solution. After 5 days, the crystal was transferred to oil, mounted in a nylon loop, and flash-cooled in a cryostream (120 K) mounted on a Rigaku FRC rotating anode. Data collection parameters are summarized in Table 2. Data were processed using DENZO and SCALEPACK.[48] Initial refinement was begun using SHELX,[49] and finally using CNS.[50] Final refinement parameters are summarized in Table 3. The coordinates have been deposited in the Protein Data Bank (PDB) with reference code 1HBJ.

Acknowledgment. This work was supported by the European Union's 4th Framework Program in Biotechnology.

References

(1) Enz, A.; Amstutz, R.; Boddeke, H.; Gmelin, G.; Malanowski, J. Brain selective inhibition of acetylcholinesterase: a novel approach to therapy for Alzheimer's disease. *Prog. Brain Res.* **1993**, *98*, 431−438.

(2) Millard, C. B.; Broomfield, C. A. Anticholinesterases: medical applications of neurochemical principles. *J. Neurochem.* **1995**, *64*, 1909−1918.

(3) Weinstock, M. Possible role of the cholinergic system and disease models. *J. Neural Transm., Suppl.* **1997**, *49*, 93−102.

(4) Lindner, A.; Schalke, B.; Toyka, K. V. Outcome in juvenile-onset myasthenia gravis: a retrospective study with long-term follow-up of 79 patients. *J. Neurol.* **1997**, *244*, 515−520.

(5) Aldridge, W. N. Some Properties of Specific Cholinesterase with Particular Reference to the Mechanism of Inhibition by Diethyl p-Nitrophenyl Thiophosphate (E605) and Analogues. *Biochem. J.* **1950**, *46*, 451−460.

(6) Davis, K. L.; Powchik, P. Tacrine. *Lancet* **1995**, *345*, 625−630.

(7) Ballantyne, B.; Marrs, T. C. *Clinical and experimental toxicology of organophosphates and carbamates*; Butterworth-Heinemann: Oxford.

(8) Sugimoto, H.; Iimura, Y.; Yamanishi, Y.; Yamatsu, K. Synthesis and structure−activity relationships of acetylcholinesterase inhibitors: 1-benzyl-4-[(5,6-dimethoxy-1-oxoindan-2-yl)methyl]-piperidine hydrochloride and related compounds. *J. Med. Chem.* **1995**, *38*, 4821−4829.

(9) Sussman, J. L.; Harel, M.; Frolow, F.; Oefner, C.; Goldman, A.; et al. Atomic structure of acetylcholinesterase from Torpedo californica: a prototypic acetylcholine-binding protein. *Science* **1991**, *253*, 872−879.

(10) Harel, M.; Quinn, D. M.; Nair, H. K.; Silman, I.; Sussman, J. L. The X-Ray Structure of a Transition State Analog Complex Reveals the Molecular Origins of the Catalytic Power and Substrate Specificity of Acetylcholinesterase. *J. Am. Chem. Soc.* **1996**, *118*, 2340.

(11) Harel, M.; Schalk, I.; Ehret-Sabatier, L.; Bouet, F.; Goeldner, M.; et al. Quaternary ligand binding to aromatic residues in the active-site gorge of acetylcholinesterase. *Proc. Natl. Acad. Sci. U.S.A.* **1993**, *90*, 9031−9035.

(12) Millard, C. B.; Kryger, G.; Ordentlich, A.; Greenblatt, H. M.; Harel, M.; et al. Crystal structures of aged phosphonylated acetylcholinesterase: nerve agent reaction products at the atomic level. *Biochemistry* **1999**, *38*, 7032−7039.

(13) Greenblatt, H. M.; Kryger, G.; Lewis, T.; Silman, I.; Sussman, J. L. Structure of acetylcholinesterase complexed with (−)-galanthamine at 2.3 A resolution. *FEBS Lett.* **1999**, *463*, 321−326.

(14) Kryger, G.; Silman, I.; Sussman, J. L. Structure of acetylcholinesterase complexed with E2020 (Aricept): implications for the design of new anti-Alzheimer drugs. *Struct. Fold. Des.* **1999**, *7*, 297−307.

(15) Harel, M.; Kleywegt, G. J.; Ravelli, R. B.; Silman, I.; Sussman, J. L. Crystal structure of an acetylcholinesterase-fasciculin complex: interaction of a three-fingered toxin from snake venom with its target. *Structure* **1995**, *3*, 1355−1366.

(16) Bourne, Y.; Taylor, P.; Marchot, P. Acetylcholinesterase inhibition by fasciculin: crystal structure of the complex. *Cell* **1995**, *83*, 503−512.

(17) Bourne, Y.; Taylor, P.; Bougis, P. E.; Marchot, P. Crystal structure of mouse acetylcholinesterase. A peripheral site-occluding loop in a tetrameric assembly. *J. Biol. Chem.* **1999**, *274*, 2963−2970.

(18) Raves, M. L.; Harel, M.; Pang, Y. P.; Silman, I.; Kozikowski, A. P.; et al. Structure of acetylcholinesterase complexed with the nootropic alkaloid, (−)-huperzine A. *Nat. Struct. Biol.* **1997**, *4*, 57−63.

(19) Gilson, M. K.; Straatsma, T. P.; McCammon, J. A.; Ripoll, D. R.; Faerman, C. H.; et al. Open "back door" in a molecular dynamics simulation of acetylcholinesterase. *Science* **1994**, *263*, 1276−1278.

(20) Axelsen, P. H.; Harel, M.; Silman, I.; Sussman, J. L. Structure and dynamics of the active site gorge of acetylcholinesterase: synergistic use of molecular dynamics simulation and X-ray crystallography. *Protein Sci.* **1994**, *3*, 188−197.

(21) Ordentlich, A.; Barak, D.; Kronman, C.; Ariel, N.; Segall, Y.; et al. Contribution of aromatic moieties of tyrosine 133 and of the anionic subsite tryptophan 86 to catalytic efficiency and allosteric modulation of acetylcholinesterase. *J. Biol. Chem.* **1995**, *270*, 2082−2091.

(22) Felder, C. E.; Botti, S. A.; Lifson, S.; Silman, I.; Sussman, J. L. External and internal electrostatic potentials of cholinesterase models. *J. Mol. Graph. Model* **1997**, *15*, 318−327, 335−317.

(23) Pang, Y. P.; Kozikowski, A. P. Prediction of the binding site of 1-benzyl-4-[(5,6-dimethoxy-1-indanon-2-yl)methyl]piperidine in acetylcholinesterase by docking studies with the SYSDOC program. *J. Comput.-Aided Mol. Des.* **1994**, *8*, 683−693.

(24) Pang, Y. P.; Kozikowski, A. P. Prediction of the binding sites of huperzine A in acetylcholinesterase by docking studies. *J. Comput.-Aided Mol. Des.* **1994**, *8*, 669−681.

(25) Cho, S. J.; Garsia, M. L.; Bier, J.; Tropsha, A. Structure-based alignment and comparative molecular field analysis of acetylcholinesterase inhibitors. *J. Med. Chem.* **1996**, *39*, 5064−5071.

(26) Kawakami, Y.; Inoue, A.; Kawai, T.; Wakita, M.; Sugimoto, H.; et al. The rationale for E2020 as a potent acetylcholinesterase inhibitor. *Bioorg. Med. Chem.* **1996**, *4*, 1429−1446.

(27) Camps, P.; Cusack, B.; Mallender, W. D.; El Achab, R. E.; Morral, J.; et al. Huprine X is a novel high-affinity inhibitor of acetylcholinesterase that is of interest for treatment of Alzheimer's disease. *Mol. Pharmacol.* **2000**, *57*, 409−417.

(28) Han, Y. F.; Li, C. P.; Chow, E.; Wang, H.; Pang, Y. P.; et al. Dual-site binding of bivalent 4-aminopyridine- and 4-aminoquinoline-based AChE inhibitors: contribution of the hydrophobic alkylene tether to monomer and dimer affinities. *Bioorg. Med. Chem.* **1999**, *7*, 2569−2575.

(29) Camps, P.; El Achab, R.; Gorbig, D. M.; Morral, J.; Munoz-Torrero, D.; et al. Synthesis, in vitro pharmacology, and molecular modeling of very potent tacrine-huperzine A hybrids as acetylcholinesterase inhibitors of potential interest for the treatment of Alzheimer's disease. *J. Med. Chem.* **1999**, *42*, 3227−3242.

(30) Kryger, G.; Silman, I.; Sussman, J. L. Three-dimensional structure of a complex of E2020 with acetylcholinesterase from Torpedo californica. *J. Physiol. Paris* **1998**, *92*, 191−194.

(31) Harel, M.; Silman, I.; Sussman, J. L. Private commmunications, later published as ref 11, 1997.

(32) Street, I. P.; Lin, H. K.; Laliberte, F.; Ghomashchi, F.; Wang, Z.; et al. Slow- and tight-binding inhibitors of the 85-kDa human phospholipase A2. *Biochemistry* **1993**, *32*, 5935−5940.

(33) Imperiali, B.; Abeles, R. H. Inhibition of serine proteases by peptidyl fluoromethyl ketones. *Biochemistry* **1986**, *25*, 3760−3767.

(34) Veale, C. A.; Bernstein, P. R.; Bohnert, C. M.; Brown, F. J.; Bryant, C.; et al. Orally active trifluoromethyl ketone inhibitors of human leukocyte elastase. *J. Med. Chem.* **1997**, *40*, 3173−3181.

(35) Neises, B.; Broersma, R. J.; Tarnus, C.; Piriou, F.; Remy, J. M.; et al. Synthesis and comparison of tripeptidylfluoroalkane thrombin inhibitors. *Bioorg. Med. Chem.* **1995**, *3*, 1049−1061.

(36) Szekacs, A.; Halarnkar, P. P.; Olmstead, M. M.; Prag, K. A.; Hammock, B. D. Heterocyclic derivatives of 3-substituted-1,1,1-trifluoro-2-propanones as inhibitors of esterolytic enzymes. *Chem. Res. Toxicol.* **1990**, *3*, 325−332.

(37) Nair, H. K.; Lee, K.; Quinn, D. M. *m*-(*N*,*N*,*N*-Trimethylammonio)trifluoroacetophenone: A femtomolar inhibitor of acetylcholinesterase. *J. Am. Chem. Soc.* **1993**, *115*, 9939−9941.

(38) Gregor, V. E.; Emmerling, M. R.; Lee, C.; Moore, C. J. The synthesis and *in vitro* acetylcholinesterase and butyrylcholinesterase inhibitory activity of Tacrine (COGNEX®) derivatives. *Bioorg. Med. Chem. Lett.* **1992**, *2*, 861−864.

(39) Desai, M. C.; Thadeio, P. F.; Lipinski, C. A.; Liston, D. R.; Spencer, R. W.; et al. Physical parameters for brain uptake: optimising LOG *P*, LOG *D* and pK_a of THA. *Bioorg. Med. Chem. Lett.* **1991**, *1*, 411−414.

(40) Gelb, M. H.; Svaren, J. P.; Abeles, R. H. Fluoro ketone inhibitors of hydrolytic enzymes. *Biochemistry* **1985**, *24*, 1813−1817.

(41) Godard, A.; Queguiner, G. o-Aminoformylquinolines, New Heterocyclic Synthons. *J. Heterocycl. Chem.* **1980**, *17*, 465−473.

(42) Krishnamurti, R.; Bellew, D. R.; Prakash, G. K. S. Preparation of Trifluoromethyl and Other Perfluoroalkyl Compounds with (Perfluoroalkyl)trimethylsilanes. *J. Org. Chem.* **1991**, *56*, 984−989.

(43) Camps, P.; El Achab, R.; Morral, J.; Munoz-Torrero, D.; Badia, A.; et al. New Tacrine-Huperzine A Hybrids (Huprines): Highly Potent Tight-Binding Acetylcholinesterase Inhibitors of Interest for the Treatment of Alzheimer's Disease. *J. Med. Chem.* **2000**, *43*, 4657−4666.

(44) Badia, A.; Banos, J. E.; Camps, P.; Contreras, J.; Gorbig, D. M.; et al. Synthesis and evaluation of tacrine-huperzine A hybrids as acetylcholinesterase inhibitors of potential interest for the treatment of Alzheimer's disease. *Bioorg. Med. Chem.* **1998**, *6*, 427−440.

(45) Barril, X.; Orozco, M.; Luque, F. J. Predicting Relative Binding Free Energies of Tacrine-Huperzine A Hybrids as Inhibitors of Acetylcholinesterase. *J. Med. Chem.* **1999**, *42*, 5110−5119.

(46) Sussman, J. L.; Harel, M.; Frolow, F.; Varon, L.; Toker, L.; et al. Purification and crystallization of a dimeric form of acetylcholinesterase from Torpedo californica subsequent to solubilization with phosphatidylinositol-specific phospholipase C. *J. Mol. Biol.* **1988**, *203*, 821−823.

(47) Ellman, G. L.; Courtney, K. D.; Andres, B. J.; Featherstone, R. M. A new and rapid colorimetric determination of acetylcholinesterase activity. *Biochem. Pharmacol.* **1961**, *7*, 88−95.
(48) Otwinowski, Z.; Minor, W. Processing of X-ray Diffraction Data Collected in Oscillation Mode. *Methods Enzymol.* **1997**, *276*, 307−326.
(49) Sheldrick, G. M.; Schneider, T. M. SHELXL: High-Resolution Refinement. *Methods Enzymol.* **1997**, *277*, 319−343.
(50) Brunger, A. T.; Adams, P. D.; Clore, G. M.; DeLano, W. L.; Gros, P.; et al. Crystallography & NMR system: A new software suite for macromolecular structure determination. *Acta Crystallogr., D* **1998**, *54*, 905−921.
(51) McRee, D. E. XtalView/Xfit--A versatile program for manipulating atomic coordinates and electron density. *J. Struct. Biol.* **1999**, *125*, 156−165.
(52) Merritt, E. A.; Bacon, D. J. Raster3D: Photorealistic molecular graphics. *Methods Enzymol.* **1997**, *277*, 505−524.

JM010826R